Celal Bayar University Journal of Science

Experimental and DFT-Based Investigation of Structural, Spectroscopic, and Electronic Features of 6-Chloroquinoline

Etem Köse[1*], Fehmi Bardak[1]

[1]Department of Physics, Faculty of Art and Sciences, Manisa Celal Bayar University, Manisa, Türkiye
*etemmm43@gmail.com
*Orcid No: 0000-0001-5791-8873

Received: 12 June 2023
Accepted: 02 September 2023
DOI: 10.18466/cbayarfbe.1313229

Abstract

This study, spectroscopic, molecular structure, and electronic features of 6-chloroquinoline were studied via experimental techniques of FT-IR, UV-Vis, ^{1}H and ^{13}C NMR and electronic structure with DFT/B3LYP method and 6-311++G(d,p) basis set combination. The modes of vibrational were assigned according to the potential energy distributions through the VEDA program. The gauge-invariant atomic orbital method was utilized to obtain nuclear magnetic resonance properties and chemical shifts and provided in comparison to the experimental data. Frontier molecular orbital properties and electronic absorption spectral properties, hence UV-Vis spectrum, were obtained by TD-DFT modeling. The compound of chemical reactivity was explored according to frontier molecular orbital properties, electrostatic potential surface characteristics, and analysis of atomic charge. It has been achieved that the chlorine substitution significantly alters the reactive nature of quinoline moiety.

Keywords: 6-chloroquinoline; DFT; IR; NMR

1. Introduction

Quinoline is heterocyclic compound with chemical formula C_9H_7N and consisting of phenyl fused with a pyridine at two adjacent carbon atoms. Applications of quinoline and its derivatives span a wide range of fields, including pharmaceuticals, agrochemicals, dyes, and organic synthesis. Biological [1–3], antifilarial [4], antibacterial [5], [6], antimalarial [7–9], cardiovascular [10], and antineoplastic [11] activities of its derivatives have been investigated widely. For instance, a quinoline derivative aminoquinoline has been tested for inhibitory potential for human immunodeficiency virus (HIV) [12]. Some of quinoline derivative has also been investigated [13–18] by using quantum chemical calculations and the spectroscopic features were presented due to their significance.

It has been revealed that the substitution in quinoline derivatives affects chemical and physical properties, such as solubility, reactivity, and biological activity. The chlorine substitution in quinoline has promising potential to alter these properties considerably because of the high electronegativity of chlorine atoms. The aforementioned points provide a general overview, but detailed studies and experimental evidence are necessary to fully understand the consequences of chlorine substitution in a particular quinoline derivative.

Therefore, this study investigated the structural characteristics, spectroscopic features, orbital interactions, electronic transitions, and nuclear magnetic resonance properties of 6-chloroquinoline (6CQ) molecules from both experimental and theoretical perspectives.

The experimental techniques utilized to reveal structural and spectroscopic features of the 6CQ are FT-IR, UV-Vis, and NMR. The electronic structure calculation performed to support experimental data by simulation the related spectra theoretically and reveal further details about the reactivity and interaction profile of the title molecules is based on DFT and Time-Dependent DFT. By examining the electronic structure and studying the theoretical spectra, this approach allowed for a more comprehensive understanding of the compound's properties and behavior. This study contributes to the existing knowledge by investigating the structural and spectroscopic characteristics of 6CQ, shedding light on its properties and potential applications. Besides, it provides a further understanding of the influence of chlorine substitution on physical and chemical properties in quinoline derivatives.

Celal Bayar University Journal of Science
Volume 19, Issue 3, 2023, p 271-281
Doi: 10.18466/cbayarfbe.1313229

2. Materials and Methods

2.1 Quantum Chemical Calculations and Spectral Data

The DFT and TD-DFT method preferred for electronic structure calculations by the Gaussian 16 program [19]. The firstly the 6CQ was fully optimized to have stable molecular geometry in the gas phase at the B3LYP method 6-311++G(d,p) basis set [20–22]. The other spectroscopic calculations were obtained with their the optimized structure. The scaled factors were used to 0.983 greater than 1700 cm^{-1} and 0.958 for up to 1700 cm^{-1} respectively, for vibrational wavenumbers, to correct overestimations [23] because of systematic errors [24]. The fundamental modes were determined in accordance with their PED (potential energy distribution) by using the VEDA program [25] and the GaussView interface [26] to have visual animation and for the verification of these modes. The GIAO method is the most prevalent approach for calculating shielding tensors and is necessary for reliable studies. So, ^{1}H and ^{13}C NMR isotropic shielding of the 6CQ were investigated by using the GIAO method [27], [28] at the same level of theory. The frontier orbitals including the highest occupied and lowest unoccupied molecules orbitals and their energies, electronic transitions, oscillator strengths, and absorbance spectrum were obtained by Time-Dependent DFT (TD-DFT) method.

The infrared spectrum of the studied molecule was used in the databank Standard Reference Data of the National Institute of Standards and Technology, NIST [30]. The ^{1}H NMR spectrum data was used in the experimental data of Spectral Database for Organic Compounds, SDBS [31].

3. Results and Discussion

3.1 Geometrical Structure

Because there is not any revealed x-ray crystallography data of 6CQ, the geometric parameters were compared with that of 2-dichloroquinoline (2DCQ), and quinoline [32], [33] to ensure the validity of electronic structure model chemistry applied in this study. **Figure 1** shows the optimized structure of 6CQ with atom numbering, and the related geometrical parameters were collated in **Table 1**.

The theoretical C–C bond lengths in the phenyl group are in the range of 1.371-1.429 Å for the B3LYP method 6-311G++(d,p) basis set. They are in good agreement with their experimental values reported between 1.358 and 1.4152 Å for quinoline [33] and 1.367 and 1.4175 Å for 2DCQ [32].

Also the bond lengths of C–C in the pyridine range from 1.372 to 1.429 Å for B3LYP with 6-311G++(d,p) basis set which is in good agreement with experimental values[32], [33]. The average deviation of bond lengths from experimental values is nearly 0.086 and 0.072 Å already for quinoline and 2DCQ molecules, respectively. Bond angle calculations also well correlated with experimental results with only averages of 0.8º and 1.9º deviations, for quinoline and 2DCQ molecules, respectively. The maximum variation, 3.4º, is observed in the C_{10}-C_4-H_{13} bond angle indicating that the N atom located as para position in this state, plays an important role in the distortion of the benzene ring despite creating no effect on bond lengths. The C-H bond lengths are in good agreement with its experimental values [32], [33]. For example, the calculated average of C-H bond lengths, 1.084 Å is in good consistent with their experimental reports of 0.984 Å and 0.95 Å for quinoline and 2DCQ molecules, respectively.

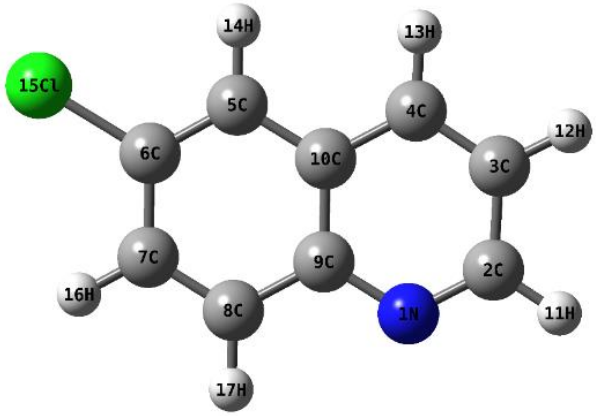

Figure 1: The optimized geometrical structure of 6CQ.

The variation, due to the substitution of the Cl atom to phenyl, in the bond length of the C_5-C_6 and C_9-C_{10} bond is 0.044 and 0.071 Å, respectively, while expecting deviations from the quinoline molecule. The deviation of bond lengths from experimental values is nearly insignificant as expected because this difference does not belong to the molecule. Bond angle calculations also well correlated with experimental results with only an average of 0.8º and 1.8º deviations for quinoline and 2DCQ molecules, respectively. Lastly, dihedral angles show clearly that the molecule is perfectly planar.

Table 1. The experimental and optimized bond lengths (Å) and angles (º) for 2-dichloroquinoline, quinoline, and 6-chloroquinoline (6CQ) molecules B3LYP/6-311++G(d,p).

Parameters	Exp.		Theory	Parameters	Exp.		Theory
Bond Lengths	2DCQ[a]	Quinoline[b]	6CQ	Bond Angles	2DCQ[a]	Quinoline[b]	6CQ
N_1-C_2	1.2959 (17)	1.319 (2)	1.315	C_6-C_5-C_{10}	120.06 (13)	120.80(14)	119.4
N_1-C_9	1.3738 (17)	1.3742 (17)	1.363	C_6-C_5-C_{14}	120.0	121.5(10)	120.7
C_2-C_3	1.4096 (18)	1.400 (3)	1.417	C_{10}-C_5-H_{14}	120.0	117.7(10)	119.9
C_2-H_{11}	1.7475 (13)	1.01 (2)	1.087	C_5-C_6-C_7	120.67 (13)	120.28(15)	121.7
C_3-C_4	1.3589 (19)	1.350 (3)	1.372	C_5-C_6-Cl_{15} (H)	119.7	122.1(11)	119.8
C_3-H_{12}	0.95	0.98 (2)	1.084	C_7-C_6-Cl_{15} (H)	119.7	117.6(11)	118.5
C_4-C_{10}	1.4225 (18)	1.414 (2)	1.417	C_6-C_7-C_8	120.38 (13)	120.47(15)	119.6
C_4-H_{13}		0.97 (2)	1.085	C_6-C_7-H_{16}	119.8	119.5(10)	119.4
C_5-C_6	1.371 (2)	1.4152 (18)	1.371	C_8-C_7-H_{16}	119.8	120.0(10)	121.0
C_5-C_{10}	1.4175 (19)	1.416 (2)	1.418	C_7-C_8-C_9	120.63 (13)	120.44(14)	120.9
C_5-H_{14}	0.95	0.95 (2)	1.083	C_7-C_8-H_{17}	119.7	122.0(10)	121.2
C_6-C_7	1.408 (2)	1.412 (2)	1.414	C_9-C_8-H_{17}	119.7	117.6(10)	117.9
C_6-Cl_{15} (H)	0.95	0.97 (2)	1.758	N_1-C_9-C_8	118.04 (12)	118.42(12)	118.6
C_7-C_8	1.367 (2)	1.365 (2)	1.373	N_1-C_9-C_{10}	122.89 (12)	122.40(12)	122.6
C_7-H_{16}	0.95	0.98(2)	1.083	C_8-C_9-C_{10}	119.07 (12)	119.17(13)	118.8
C_8-C_9	1.4114 (19)	1.410(2)	1.419	C_4-C_{10}-C_5	124.81 (12)	122.1(11)	122.9
C_8-H_{17}	0.95	1.03(2)	1.083	C_4-C_{10}-C_9	116.01 (12)	117.32(13)	117.5
C_9-C_{10}	1.4217 (19)	1.358(2)	1.429	C_5-C_{10}-C_9	119.18 (12)	118.83(13)	119.6
Bond Angles (º)				Selected Dihedral Angles (º)			
C_2-N_1-C_9	116.14 (13)	116.71 (11)	117.9	C_9-N_1-C_2-C_3		-	0
N_1-C_2-C_3	126.50 (12)	124.48(16)	124.1	C_9-N_1-C_2-H_{11}		-	180
N_1-C_2-H_{11}	116.73 (10)	116.6(11)	116.3	C_2-N_1-C_9-C_8		-	180
C_3-C_2-H_{11}	116.77 (10)	118.9(11)	119.6	C_2-N_1-C_9-C_{10}		-	0
C_2-C_3-C_4	116.60 (12)	118.95(16)	118.9	N_1-C_2-C_3-C_4		-	0
C_2-C_3-H_{12}	121.7	119.4(10)	119.8	N_1-C_2-C_3-H_{12}		-	180
C_4-C_3-H_{12}	121.7	121.7(10)	121.4	C_{10}-C_5-C_6-Cl_{15}		-	180
C_3-C_4-C_{10}	121.26 (12)	119.83(15)	119.2	H_{14}-C_5-C_6-Cl_{15}		-	0
C_3-C_4-H_{13}	-	124.0(10)	121.2	C_3-C_4-C_{10}-C_5		-	180
C_{10}-C_4-H_{13}	-	116.2(10)	119.6	C_6-C_5-C_{10}-C_9		-	0

[a] The X-Ray data from ref [32]
[b] The X-Ray data from ref [33]

3.2 Vibrational Spectral Analysis

The vibrational analysis was prepared as theoretical by using DFT/B3LYP/6-311G++(d,p) model chemistry and compared the experimental data belonging to the 6CQ and the similar structural molecules. The title molecule has C_s symmetry and has 45 fundamental vibrational modes that can be distributed as 31A' + 14A" in which A" and A' represent the out-of-plane and in-plane modes, respectively. The experimental and theoretical IR spectra of 6CQ are given in **Figure 2** and the proposed vibrational assignments generated through PED calculation and visual examination via the GaussView6 program are gathered in **Table 2.** Last column presents a description of detailed fundamental modes. The results of the theory obtained by the B3LYP method and 6-311++G (d,p) basis set. The frequencies of vibrational spectra obtained through electronic structure calculations are generally higher than that from experimental results because the calculations are based on single molecule either in vacuum or in polarizable continuum model (PCM) whereas the experiments conducted in solid phase. Besides, the theoretical calculations are obtained at the lowest energy equilibrium geometry and the anharmonic behaviors are omitted to avoid the calculational expense.

The C–H stretching modes of organic molecules are generally observed as multiple peaks in the region of 3000–3100 cm^{-1} [34]. In this study, we observed (ν_1–ν_6) in the range of 3006–3070 cm^{-1} and calculated in the range of 3010–3072 cm^{-1} as pure modes by B3LYP functional of DFT as seen PED column in **Table 2.** The C-H symmetric vibrations modes have higher wavelengths than asymmetric ones in rings.

Celal Bayar University Journal of Science
Volume 19, Issue 3, 2023, p 271-281
Doi: 10.18466/cbayarfbe.1313229

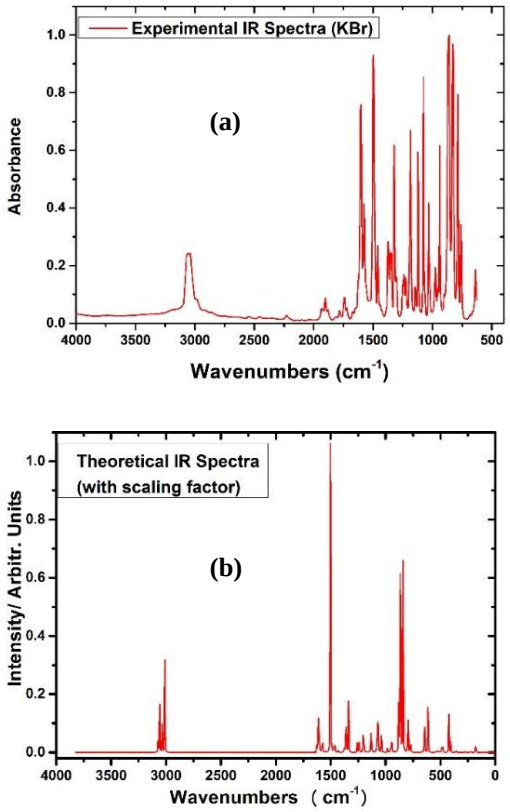

Figure 2. The experimental (a) and theoretical (b) IR spectra of 6CQ.

The in-plane and out-of-plane bending modes of C–H are generally observed in aromatic compounds in the range of 1000–1300 cm^{-1} and 750–1000 cm^{-1}, respectively [35]. The experimental C–H in-plane bending modes of the studied molecule are in the range of 1032–1497 cm^{-1} and generally mixed with C–C and C–N stretching modes according to their PED results. The C–H out-of-plane bending vibrations were found at 873, 946–976 cm^{-1} region.

The stretching vibrations modes of C–N are generally very difficult to determine due to the mixing of other modes. Silverstein et al. [36] defined the C–N stretching modes in the region of 1386–1266 cm^{-1} for aromatic amines. The modes are very broadband and mixed with the C–C modes, the biggest contribution of C–N vibrations comes from mode ν_{15} according to the PED analysis. The scaled wavelengths of C–N are well correlating with experimental observations. The results have also good similarity for similar quinoline derivatives[13], [37], [38].

Two or three bands were recorded in the region 1600–1200 cm^{-1} named skeletal vibrations modes.

The most conurbations generally at about 1500 cm^{-1} for six-membered aromatic rings like phenyl and pyridine. Varsányi [39] also recorded five bands at 1625–1590, 1590–1575, 1540–1470, 1465–1430, and 1380–1280 cm^{-1} and implied that these bands are of variable intensity. In this study, C–C stretching vibrations modes were dedicated in the region 1032–1621, 941, 859, 766, 607, 516, 417, and 218 cm^{-1} and overlapped the other stretching modes. The highest percentages of PED were obtained as 61%, and 64%, for υ7 and υ22 modes, respectively. The results of the C–C stretching modes are in good correlation with the experimental vibrational results. C–C stretching modes are also well correlated for similar structural molecules in the literature[37], [40], [41].

The stretching vibrations of C-Cl are recorded generally as broad bands region at 760-505 cm^{-1} [42]. The C-Cl stretching modes of the 1-chloroisoquinoline molecule were identified at 675 cm^{-1} and at 674 cm^{-1}, FT-Raman and FT-IR bands respectively [43]. Also, the C-Cl stretching modes of 8CQ were recorded as a very strong band at 659 and 651 cm^{-1} in IR and Raman, respectively [13]. The C-Cl stretching vibrations that appeared at 355 and 589 cm^{-1} show a deviation due to nitrogen atoms with electro-negative properties [37]. In the present work, the C-Cl stretching modes of the 6CQ molecule were observed at 351, 607, and 637 cm^{-1} and showed a good correlation with the experimental results, and literature. The experimental and theoretical correlation of vibrational frequencies can be seen from **Figure 3**.

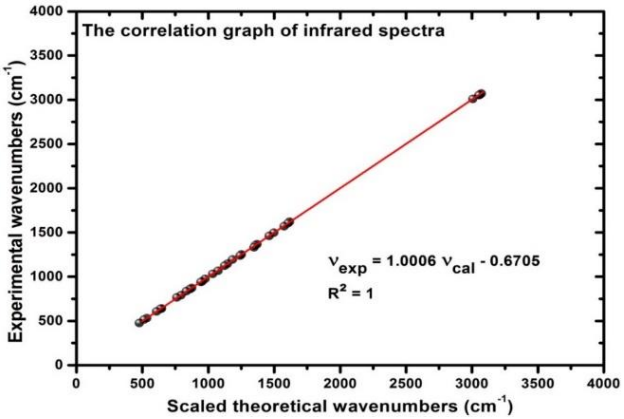

Figure 3. The correlation of the of 6CQ molecule for IR spectra.

Table 2. The calculated and experimental (FT-IR) wavenumbers (cm^{-1}) using B3LYP method 6-311++G(d,p) basis set of 6CQ molecule.

Modes No	Sym.	Theoretical		Experimental		PED[b] (≥10%)
		Unscaled freq.	Scaled freq.[a]	FT-IR$_{nujol}$	FT-IR$_{KBR}$	
ν1	A'	3206	3072	3070		$\nu CH_{sym.}$ (100)
ν2	A'	3192	3058	3059		$\nu CH_{sym.}$ (99)
ν3	A'	3191	3057	3056		$\nu CH_{asym.}$ (100)
ν4	A'	3188	3054		3052	$\nu CH_{asym.}$ (99)
ν5	A'	3166	3033			$\nu CH_{asym.}$ (100)
ν6	A'	3142	3010	3006		$\nu CH_{asym.}$ (100)
ν7	A'	1649	1621	1616		νCC (61), δCCH (21), δCCC (13)
ν8	A'	1632	1604	1595	1604	νCC (46), νCN (19), δCCH (16), δCCC (10)
ν9	A'	1598	1571	1566	1574	νCC (39), νCN (16), δCCC (31)
ν10	A'	1523	1497	1491	1496	νCC (29), νCN (10), δCCH (41), δCCN (13)
ν11	A'	1487	1461	1454	1461	νCC (27), δCCH (44), δCCN (10), δCCC (10)
ν12	A'	1451	1427			νCC (22), δCCH (65)
ν13	A'	1392	1368	1369	1372	νCC (48), νCN (11), δCCC (26), δCCH (12)
ν14	A'	1377	1354	1355	1356	νCC (47), νCN (18), δCCH (31)
ν15	A'	1356	1333	1347	1346	νCC (15), νCN (28), δCCH (36), δCCC (14)
ν16	A'	1274	1252	1250	1251	νCC (18), δCCH (57), δCCC (14)
ν17	A'	1260	1239	1241	1240	νCC (21), νCN (13), δCCH (46), δCCC (10)
ν18	A'	1215	1195	1184	1183	νCC (18), δCCH (72)
ν19	A'	1166	1146	1145	1144	νCC (29), δCCH (66)
ν20	A'	1144	1125	1120	1123	νCC (31), δCCH (38), δCCC (16), δCCN (10),
ν21	A'	1085	1067	1074	1073	νCC (40), νCN (13), δCCH (22), δCCC (14)
ν22	A'	1050	1032	1033	1032	νCC (64), δCCH (26)
ν23	A"	993	976	980	975	γCH [τCCCH (78), τCCCN (18)]
ν24	A"	983	967	959		γCH [τCCCH (73), τCCCN (24)]
ν25	A"	963	946		952	γCH [τCCCH (70), τCCCN (21)]
ν26	A'	957	941	943	940	νCC (11), δCCH (14), δCCC (54), δCCN (10)
ν27	A"	888	873	874		γCH [τCCCH(89), τCCCN (10)]
ν28	A'	874	859	854	860	νCC (11), δCCC (52), δCCN (21)
ν29	A"	850	836	832	828	γCH [τCCCH(90)]
ν30	A"	804	790	792	787	γCH [τCCCH(25), τCCCN (61), τCCCC (12)]
ν31	A"	779	766	766		νCC (19), νCN (13), δCCN (30), δCCH (11), δCCC (23)
ν32	A'	779	765		760	γCH [τCCCH (78), τCCCN (12)]
ν33	A'	651	640	645		γCH [τCCCH(21), τCCCN(38), τCCCC(15)], τCNCCl (25)
ν34	A"	648	637		637	νCC (22), νCCl (10), δCCN (25), δCCH (14), δCCC (24)
ν35	A'	618	607	607		νCC (14), νCCl (19), δCCN (11), δCCC (45)
ν36	A'	540	531	532		γCH [τCCCH(21), τCCCN(38), τCCCC(18)], τCNCCl (21)
ν37	A"	525	516	512		νCC (23), δCCN (16), δCCH (21), δCCC (36)
ν38	A"	485	477	476		γCH [τCCCH(14), τCCCN (67), τCCCC (14)]
ν39	A'	425	417			νCC (19), δCNCl (22), δCCC (45)
ν40	A"	408	401			γCH [τCCCH(14), τCCCN (73), τCCCC (11)]
ν41	A'	357	351			νCN (10), νCCl (49), δCCH (10), δCCC (15)
ν42	A"	274	269			τCCCN (60), τCNCCl (25), τCCCC (11)
ν43	A'	221	218			νCC (12), δCNCl (61), δCCC (16)
ν44	A"	174	171			τCCCN (95)
ν45	A"	101	99			τCCCN (67), τCNCCl (16)

[a] The scale factor used to 0.958 and 0.983 ranges from 4000 to 1700 cm^{-1} and lower than 1700 cm^{-1}, respectively.
[b] Potential Energy Distribution; PED, ν; stretching, γ; out-of plane bending, δ; in-plane-bending, τ; torsion, ρ; scissoring, ω; wagging, φ; twisting, ρ; rocking.

Celal Bayar University Journal of Science
Volume 19, Issue 3, 2023, p 271-281
Doi: 10.18466/cbayarfbe.1313229

3.3 Nuclear Magnetic Resonance Spectra

NMR spectra is a principal method for studying of organic molecules. The NMR spectroscopic results, recorded with computer simulation methods, help to have more information about the structure of biomolecules as a strong method [27], [28]. The Gauge-including atomic orbital (GIAO) [27], [28] method at B3LYP method 6-311G++(d,p) level theory is used to obtain ^{1}H and ^{13}C NMR spectra of 6CQ molecule after full optimization of its geometry. The theoretical (gas phase and in $CDCl_3$) and experimental data (in $CDCl_3$)[31] of ^{1}H and ^{13}C NMR spectra were gathered in **Table 3**. **Figure 4a-4b** present the taken experimental spectra [31] of ^{1}H and ^{13}C NMR of the studied molecule.

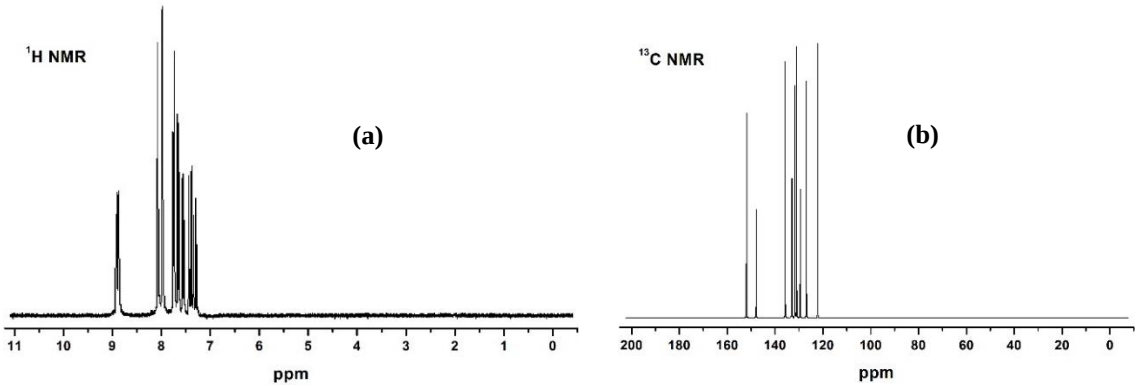

Figure 4. (a) The experimental ^{1}H and (b) ^{13}C NMR spectra of 6CQ

Table 3. Theoretical and experimental ^{1}H and ^{13}C NMR chemical shifts of 6CQ molecule B3LYP method 6-311++ G(d,p)) basis set.

Atoms	Exp. ($CDCl_3$)	Teo. $CDCl_3$	Teo. Gas
C_2	150.51	156.07	155.08
C_3	121.79	126.39	125.35
C_4	134.93	140.53	138.80
C_5	126.32	131.33	130.47
C_6	132.18	146.26	147.15
C_7	130.26	134.94	134.69
C_8	131.06	137.17	137.63
C_9	146.57	153.27	153.56
C_{10}	128.71	134.13	133.84
H_{11}	8.89	9.11	9.07
H_{12}	7.39	7.58	7.36
H_{13}	8.03	8.29	8.04
H_{14}	7.76	8.00	7.82
H_{16}	7.63	7.90	7.80
H_{17}	8.03	8.25	8.24

It can be assumed that the quinoline ring contains a phenyl and a pyridine ring. The signal of protons in the phenyl ring is often observed in the range of 7–8.5 ppm. Electron withdrawing atoms or groups of atoms can reduce shielding and move the resonance to a higher frequency, while in electron donating systems it drops to a lower frequency. [44]. The H_{12} atom has appeared to have the lowest chemical shifts (δ = 7.39 ppm) and the H_{11} atom is at the highest chemical shifts (δ = 8.89 ppm) due to shielding by electronegative nitrogen atom [31].

Theoretical calculations obtained under PCM give slightly higher chemical shifts in comparison to both gas phase calculations and the experimental data. However, the correlation between experimental data and PCM modeling is better than the accordance between gas phase calculations and the measured ones.

The chemical shifts of carbons especially show resonance and overlap in the region at 100-150 ppm [45], [46] and also seen same region for quinoline in the literature [47], [48]. The shifts for carbons C_2, and C_9 are higher than the others which can be due to the neighboring nitrogen atom. The difference of the carbon NMR value of C_2 atom is reasonable as 150.51 ppm (exp.) and 156.07 ppm (calc.), similar correlations are seen the other carbons. A general correlation evaluation between the theoretical and experimental chemical shifts is given in **Figure 5**.

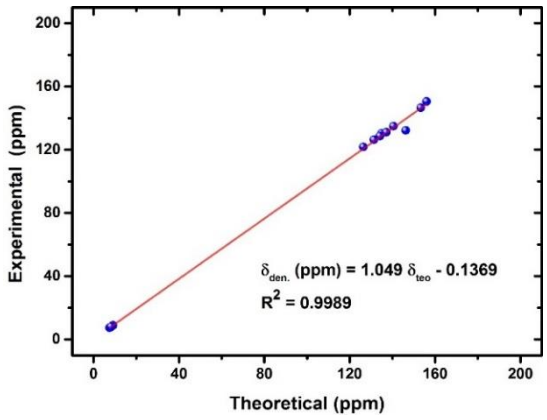

Figure 5. The correlation graphic of NMR spectra for 6CQ molecule.

Celal Bayar University Journal of Science
Volume 19, Issue 3, 2023, p 271-281
Doi: 10.18466/cbayarfbe.1313229

3.4 UV-Vis Spectra and Frontier Molecular Orbital Analysis

UV-Vis spectra were presented in gas phase, water and ethanol solvents as a theoretically to understand electronic transitions and predict the UV-Vis spectrum of 6CQ. TD–DFT method was utilized confidently because of its computational plausibility and validity for medium size molecules [49–51]. The absence of experimental data quantum chemical calculations can be useful to shed light on the literature and contribute to future studies. Theoretical electronic absorption properties were obtained using the TD–DFT method B3LYP/6-311++G(d,p) basis set. The results of UV-Vis (electronic absorption) spectra of the 6CQ molecule were graphed in **Figure 6**. The excitation energies (E), calculated absorption (λ), oscillator strength (f), and major contributions, obtained via GaussSum 2.2 [29] program, for the 6CQ, are given in **Table 4** for the gas phase, ethanol, and water solvents. The maximum wavelengths were obtained at about 290 nm for all solvents. The excitation properties chemical reactivity behavior, spectroscopic features, and the ability of electron transport were obtained by using the frontier molecular orbital (MO) determination [52]. The electron donating and accepting form of molecule can be described by highest occupied molecular orbital (HOMO) and lowest unoccupied molecular orbital (LUMO), respectively. The frontier molecular orbitals isosurface, energy gaps, and orbital transitions were listed in **Table 5** and pictured in **Figure 7**. The MO diagrams were given in **Figure 8**, to see energy levels.

The energy gaps for the gas phase, water, and solvents were obtained as 4.74, 4.77, and 4.77 eV, respectively. The red and green nodes in **Figure 7** are positive and negative values of frontier molecular orbitals. The orbital distribution of HOMO localized all regions except some hydrogen atoms. The orbital distribution of LUMO is changed on all atoms on the molecule. The other important energy gaps rather than HOMO, LUMO such as H–1→L, H→L+1, H-1→L+1, and H→L+2 (also the others) can be critical parameters in determining molecular electrical transport properties (see **Table 5** and **Figure 7**).

.

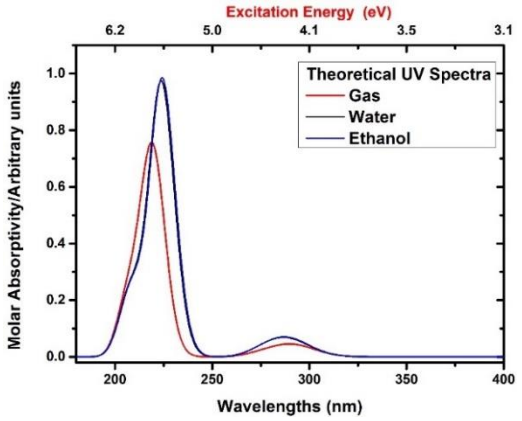

Figure 6. The theoretical UV-Vis spectra of 6CQ molecule gas phase, in ethanol and water.

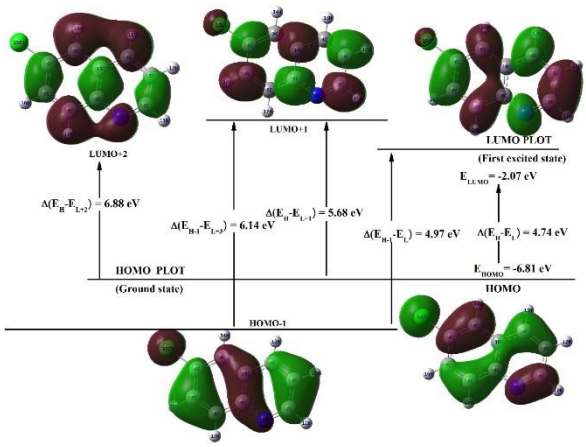

Figure 7. The remarkable FMOs of 6CQ molecule with energy gaps.

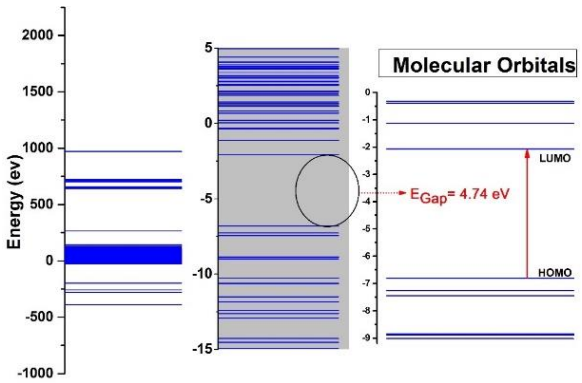

Figure 8. The MO energy levels of the 6CQ molecule.

Table 4. Experimental and calculated wavelengths λ (nm), excitation energies (eV), oscillator strengths *(f)* of 6CQ for gas phase, in ethanol and water solutions.

	TD-DFT			
	f	Major contributes	E (eV)	λ (nm)
Gas	0.0479	H→L (79%)	4.2421	292.31
	0.4897	H-1→L (13%), H-1→L+1 (16%), H→L+1 (38%), H→L+2 (21%)	5.6480	219.55
	0.2252	H-5→L (11%), H-1→L+1 (56%), H→L+2 (21%)	5.9421	208.68
Water	0.0641	H→L (81%)	4.2679	290.54
	1.2232	H-1→L (29%), H→L+1 (64%)	5.5413	223.77
	0.2591	H-1→L+1 (62%), H→L+2 (25%)	5.9114	209.76
Ethanol	0.0658	H→L (81%)	4.2646	290.77
	1.2389	H-1→L (29%), H→L+1 (64%)	5.5306	224.21
	0.2618	H-1→L+1 (62%), H→L+2 (25%)	5.9068	209.93

H: HOMO, L: LUMO

Table 5. The calculated energy values of 6CQ molecule using B3LYP 6-311++G(d,p) basis set.

TD-DFT/B3LYP/6-311++G(d,p)	Gas	Ethanol	Water
E_{total} (Hartree)	-861.49846	-900.83420	-861.50292
E_{HOMO-5} (eV)	-9.02	-9.08	-9.09
E_{HOMO-1} (eV)	-7.27	-7.26	-7.26
E_{HOMO} (eV)	-6.81	-6.83	-6.83
E_{LUMO} (eV)	-2.07	-2.06	-2.06
E_{LUMO+1} (eV)	-1.13	-1.12	-1.12
E_{LUMO+2} (eV)	-0.39	-0.37	-0.38
E_{LUMO+3} (eV)	-0.32	-0.16	-0.16
$E_{HOMO-1–LUMO\ gap}$ (eV)	5.20	5.20	5.20
$E_{HOMO-1–LUMO+1\ gap}$ (eV)	6.14	6.14	6.14
$E_{HOMO-1–LUMO+2\ gap}$ (eV)	6.88	6.89	6.88
$E_{HOMO-1–LUMO+3\ gap}$ (eV)	6.95	7.10	7.10
$E_{HOMO–LUMO\ gap}$ (eV)	4.74	4.77	4.77
$E_{HOMO–LUMO+1\ gap}$ (eV)	5.68	5.71	5.71
$E_{HOMO–LUMO+2\ gap}$ (eV)	6.42	6.46	6.45
$E_{HOMO–LUMO+3\ gap}$ (eV)	6.49	6.67	6.67
Chemical hardness (η)	-2.37	-2.39	-2.39
Electronegativity (χ)	4.44	4.45	4.45
Chemical potential (μ)	-4.44	-4.45	-4.45
Electrophilicity index (ω)	-4.16	-4.14	-4.14

The chemical potential (μ), and hardness (η) by $\mu=-(I-H)/2$, and $\eta=(I-H)/2$ in these equations I and H are ionization potential and electron affinity, were determined by Parr and Pearson [53]. Also, global electrophilicity index (ω), expressed, $\omega=\mu^2/2\eta$, in terms of μ and η [54]. The chemical hardness of molecules indicates that a hard or soft molecule according to the energy gaps, has large or small, respectively. Also, the soft molecules have more polarizable than the hard molecules because they can be excited through small excitation energies. The chemical reactivity values for 6CQ are nearly the same for gas phase and solvents indicating that the solvent does not significantly alters the chemical reactivity of the compound.

Celal Bayar University Journal of Science
Volume 19, Issue 3, 2023, p 271-281
Doi: 10.18466/cbayarfbe.1313229

3.5 Molecular Electrostatic Potential Surface

The molecular electrostatic potential surfaces (MEPs) of molecules generally provide more information about the reactive behavior of a compound because it is related to their electron density describing nucleophilic and electrophilic regions, as negative and positive, respectively [55], [56]. The counter map and three-dimensional electrostatic potential mapped electron density surface (MEP) of the studied molecule were given in **Figure 9**. The values on MEP surfaces increase from red to blue color and line up between $-4.046e^{-2}$ to $4.046e^{-2}$ (a.u.). The MEPs picture indicates that while regions with negative potential are over the electronegative nitrogen and chloride atoms, the positive ones are over the hydrogen atoms, especially H_{12} and H_{13}. The lowest negative value and highest positive potential indicate electron-rich and deficient surfaces, respectively. The MEP surface also indicates the steric center of phenyl and pyridine rings. The MEP surface is a qualitative representation of the charge distribution of the atoms in a molecule.

3.6 The Mulliken Atomic Charges

The quantum mechanical calculations of the molecular systems can generate a quantitative assignment of partial atomic charges through several types of population analysis techniques in which the most used is Mulliken population analysis. [57]. The Mulliken atomic charges of quinoline and 6CQ molecules were predicted at DFT/B3LYP method 6-31G(d) level rather than with a 6-311++G(d,p) basis set to have more reliable results. It has been observed that the large basis sets with diffusive character create an increased overlap of electron densities and causes some systematical error [37], [58]. The Mulliken atomic charges of 6CQ are given in **Figure 10** in comparison to that of Quinoline. The chloride atom creates a significant change in the charge distribution and nearby atoms due to its strong electronegative character. The charge redistribution mostly takes place among the chloride atom and the carbon atoms, and the charge of hydrogen atoms in Quinoline and 6CQ have almost the same. The hydrogen atoms are partially positive in both cases and act as electrophilic sites of the molecules.

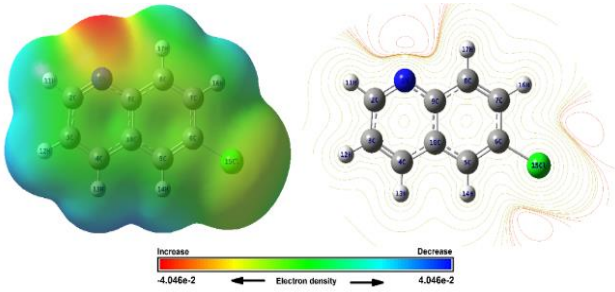

Figure 9. The molecular electrostatic potential (MEPs) surface graph for 6CQ molecule.

Significant changes occur in the partial charges of the carbon atoms in which the sign of charges of C_2, C_9, and C_{10} atoms changed from negative to positive and that of C_5 and C_6 atoms shows a change from positive to negative. This alteration is most likely caused by the strong electronegative substitution.

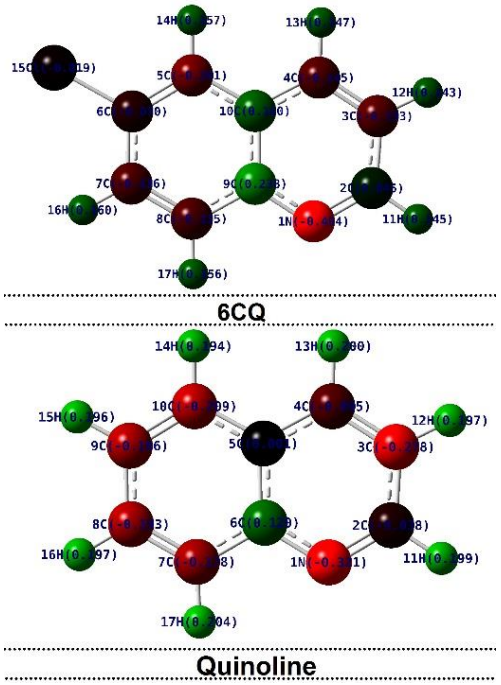

Figure 10. The Mulliken charge distribution for Quinoline and 6CQ molecules obtained through DFT/B3LYP method 6-31G(d) level model chemistry.

4. Conclusion

In conclusion, our study shows that the electronic structure and spectroscopic properties of 6-chloroquinoline have been successfully simulated using the DFT/B3LYP method and 6-311++G(d,p) basic set model chemistry. The high accuracy achieved in the theoretical simulation is supported by the perfect match with the experimental FT-IR and NMR spectroscopic data. Analysis of frontier molecular orbitals and reactivity parameters provides valuable information about the observed spectral peaks found to originate from various orbital transitions with similar probabilities. The addition of a chlorine substituent significantly affects the vibrational and chemical shielding properties of neighboring atoms within two bond distances. Moreover, the strong correlation between the simulated and observed spectra highlights the reliability and accuracy of our computational approach. In this study, it is seen that the effect of the chlorine atom is effective on both the spectroscopic and electronic properties when viewed easily in terms of the quinol molecule. The binding of halogens such as chlorine and/or fluorine attached to the quinol molecule may produce similar results.

In addition, it can be predicted that both chlorine and other halogens may be effective in spectroscopic and electronic studies for different quinol derivatives. These findings contribute to a comprehensive understanding of the electronic and spectroscopic properties of 6-chloroquinoline and pave the way for future research in this area.

References

[1] R. Gupta, A. K. Gupta, S. Paul, and P. L. Kachroo, "Synthesis and biological activities of some 2-chloro-6/8-substituted-3-(3-alkyll aryl-5, 6-dihydro-s-triazolo-[3, 4-h][1, 3, 4] thiadiazol-6-yl) quinolines," *Indian J. Chem.*, vol. 37B, pp. 1211–1213, 1998.

[2] R. Gupta, A. K. Gupta, S. Paul, and P. Somal, "Microwave-assisted synthesis and biological activities of some 7/9-substituted-4-(3-alkyl/aryl-5, 6-dihydro-s-triazolo [3, 4-b][1, 3, 4] thiadiazol-6-yl) tetrazolo [1, 5-a] quinolines," *Indian J. Chem.*, vol. 39B, pp. 847–852, 2000.

[3] D. Dubé *et al.*, "Quinolines as potent 5-lipoxygenase inhibitors: Synthesis and biological profile of L-746,530," *Bioorganic Med. Chem. Lett.*, vol. 8, no. 10, pp. 1255–1260, 1998, doi: 10.1016/S0960-894X(98)00201-7.

[4] S. Tewari, P. M. S. Chauhan, A. P. Bhaduri, N. Fatima, and R. K. Chatterjee, "Syntheses and antifilarial profile of 7-chloro-4(substituted amino) quinolines: A new class of antifilarial agents," *Bioorganic Med. Chem. Lett.*, vol. 10, no. 13, pp. 1409–1412, 2000, doi: 10.1016/S0960-894X(00)00255-9.

[5] M. Fujita, K. Chiba, Y. Tominaga, and K. Hino, "7-(2-Aminomethyl-1-azetidinyl)-4-oxoquinoline-3-carboxylic Acids as Potent Antibacterial Agents: Design, Synthesis, and Antibacterial Activity.," *Chem. Pharm. Bull.*, vol. 46, no. 5, pp. 787–796, 1998, doi: 10.1248/cpb.46.787.

[6] M. Kidwai, K. R. Bhushan, P. Sapra, R. K. Saxena, and R. Gupta, "Alumina-supported synthesis of antibacterial quinolines using microwaves," *Bioorganic Med. Chem.*, vol. 8, no. 1, 2000, doi: 10.1016/S0968-0896(99)00256-4.

[7] J. Ziegler, R. Linck, and D. W. Wright, "Heme aggregation inhibitors: Antimalarial drugs targeting an essential biomineralization process," *Stud. Nat. Prod. Chem.*, vol. 25, pp. 327–366, 2001, doi: 10.1016/S1572-5995(01)80011-9.

[8] F. M. D. Ismail, M. J. Dascombe, P. Carr, S. A. M. Mérette, and P. Rouault, "Novel aryl-bis-quinolines with antimalarial activity in-vivo," *J. Pharm. Pharmacol.*, vol. 50, no. 5, pp. 483–492, 1998, doi: 10.1111/j.2042-7158.1998.tb06189.x.

[9] O. Famin, M. Krugliak, and H. Ginsburg, "Kinetics of inhibition of glutathione-mediated degradation of ferriprotoporphyrin IX by antimalarial drugs," *Biochem. Pharmacol.*, vol. 58, no. 1, pp. 59–68, 1999, doi: 10.1016/S0006-2952(99)00059-3.

[10] K. M. Khan *et al.*, "Syntheses and cytotoxic, antimicrobial, antifungal and cardiovascular activity of new quinoline derivatives," *Arzneimittelforschung*, vol. 50, no. 10, pp. 915–924, 2000, doi: 10.1055/s-0031-1300313.

[11] L. W. Deady, J. Desneves, A. Kaye, G. Finlay, B. Baguley, and W. Denny, "Positioning of the carboxamide side chain in 11-oxo-11H-indeno[1,2-b]quinolinecarboxamide anticancer agents: Effects on cytotoxicity," *Bioorganic Med. Chem.*, vol. 9, no. 2, pp. 445–452, 2001, doi: 10.1016/S0968-0896(00)00264-9.

[12] L. Strekowski *et al.*, "Synthesis and Quantitative Structure-Activity Relationship Analysis of 2-(Aryl or Heteroaryl)quinolin-4-amines, a New Class of Anti-HIV-1 Agents," *J. Med. Chem.*, vol. 34, no. 5, pp. 1739–1746, 1991, doi: 10.1021/jm00109a031.

[13] V. Arjunan, P. Ravindran, T. Rani, and S. Mohan, "FTIR, FT-Raman, FT-NMR, ab initio and DFT electronic structure investigation on 8-chloroquinoline and 8-nitroquinoline," *J. Mol. Struct.*, vol. 988, no. 1, pp. 91–101, 2011, doi: 10.1016/j.molstruc.2010.12.032.

[14] V. Arjunan, I. Saravanan, P. Ravindran, and S. Mohan, "Ab initio, density functional theory and structural studies of 4-amino-2-methylquinoline.," *Spectrochim. Acta. A. Mol. Biomol. Spectrosc.*, vol. 74, no. 2, pp. 375–84, Oct. 2009, doi: 10.1016/j.saa.2009.06.028.

[15] S. Sivaprakash, S. Prakash, S. Mohan, and S. P. Jose, "Molecular structure, vibrational analysis (IR and Raman) and quantum chemical investigations of 1-aminoisoquinoline," *J. Mol. Struct.*, vol. 1149, pp. 835–845, 2017, doi: 10.1016/j.molstruc.2017.08.060.

[16] G. Oanca, J. Stare, A. G. Todirascu, D. Creanga, and D. O. Dorohoi, "Substituent influence on the spectra of some benzo[f]quinoline derivatives," *J. Mol. Struct.*, vol. 1126, pp. 158–164, Dec. 2016, doi: 10.1016/J.MOLSTRUC.2016.03.072.

[17] M. Kumru, A. Altun, M. Kocademir, V. Küçük, T. Bardakçı, and B. Şaşmaz, "Combined experimental and quantum chemical studies on spectroscopic (FT-IR, FT-Raman, UV–Vis, and NMR) and structural characteristics of quinoline-5-carboxaldehyde," *J. Mol. Struct.*, vol. 1125, pp. 302–309, 2016, doi: 10.1016/j.molstruc.2016.06.066.

[18] V. Arjunan, S. Mohan, P. S. Balamourougane, and P. Ravindran, "Quantum chemical and spectroscopic investigations of 5-aminoquinoline," *Spectrochim. Acta Part A Mol. Biomol. Spectrosc.*, vol. 74, no. 5, pp. 1215–1223, 2009, doi: 10.1016/j.saa.2009.09.039.

[19] M. J. Frisch *et al.*, "Gaussian 16 Revision A.03." Gaussian, Inc., Wallingford, CT, 2016.

[20] J. P. Perdew and Y. Wang, "Accurate and simple analytic representation of the electron-gas correlation energy," *Phys. Rev. B*, vol. 45, no. 23, pp. 13244–13249, Jun. 1992, [Online]. Available:http://link.aps.org/doi/10.1103/PhysRevB.45.13244.

[21] C. Lee, W. Yang, and R. G. Parr, "Development of the Colle-Salvetti correlation-energy formula into a functional of the electron density," *Phys. Rev. B*, vol. 37, no. 2, pp. 785–789, Jan. 1988, [Online]. Available: http://link.aps.org/doi/10.1103/PhysRevB.37.785.

[22] A. D. Becke, "Density-functional thermochemistry. III. The role of exact exchange," *J. Chem. Phys.*, vol. 98, no. 7, pp. 5648–5652, 1993, doi: 10.1063/1.464913.

[23] N. Sundaraganesan, S. Ilakiamani, H. Saleem, P. M. Wojciechowski, and D. Michalska, "FT-Raman and FT-IR spectra, vibrational assignments and density functional studies of 5-bromo-2-nitropyridine.," *Spectrochim. Acta Part A Mol. Biomol. Spectrosc.*, vol. 61, no. 13–14, pp. 2995–3001, Oct. 2005, doi: 10.1016/j.saa.2004.11.016.

[24] J. B. Foresman and A. Frisch, "Exploring chemistry with electronic structure methods, 1996," *Gaussian Inc, Pittsburgh, PA*, pp. 98–99, 1996.

[25] M. H. Jamróz, "Vibrational energy distribution analysis (VEDA): scopes and limitations.," *Spectrochim. Acta Part A Mol. Biomol. Spectrosc.*, vol. 114, pp. 220–230, Oct. 2013, doi: 10.1016/j.saa.2013.05.096.

[26] R. Dennington, T. Keith, and J. Millam, *GaussView, Version 5*. 2009.

[27] R. Ditchfield, "Molecular Orbital Theory of Magnetic Shielding and Magnetic Susceptibility," *J. Chem. Phys.*, vol. 56, no. 11, pp. 5688–5691, 1972, doi: 10.1063/1.1677088.

[28] K. Wolinski, J. F. Hinton, and P. Pulay, "Efficient implementation of the gauge-independent atomic orbital method for NMR chemical shift calculations," *J. Am. Chem. Soc.*, vol. 112, no. 23, pp. 8251–8260, Nov. 1990, doi: 10.1021/ja00179a005.

[29] N. M. O'Boyle, A. L. Tenderholt, and K. M. Langner, "Software News and Updates cclib : A Library for Package-Independent Computational Chemistry Algorithms," *J. Comput. Chem.*, vol. 29, no. 5, pp. 839–845, 2008, doi: 10.1002/jcc.20823.

[30] NIST Web: http://cccbdb.nist.gov/vibscalejust.asp, "http://cccbdb.nist.gov/vibscalejust.asp," 2018. .

[31] SDBS Web: http://sdbs.riodb.aist.go.jp (National Institute of Advanced Industrial Science and Technology), "SDBS Web: http://sdbs.riodb.aist.go.jp (National Institute of Advanced Industrial Science and Technology)," 2018. http://sdbs.db.aist.go.jp/sdbs/cgi-bin/direct_frame_top.cgi.

[32] R. Kimmel, M. Nečas, and R. Vícha, "2,4-Dichloroquinoline," *Acta Crystallogr. Sect. E Struct. Reports Online*, vol. 66, no. 6, pp. o261–o1261, 2010, doi: 10.1107/S160053681001576X.

[33] J. E. Davies and A. D. Bond, "Quinoline," *Acta Crystallogr. Sect. E*, vol. 57, no. 10, pp. 947–949, Oct. 2001, [Online]. Available: https://doi.org/10.1107/S1600536801014891.

[34] G. Socrates, *Infrared and Raman Characteristic Group Frequencies: Tables and Charts*. West Sussex, England: John Wiley & Sons Ltd., 2001.

[35] R. M. Silverstein, F. X. Webster, and D. J. Kiemle, *Spectrometric identification of organic compounds*. John Wiley & Sons, 2005.

[36] R. M. Silverstein, G. C. Bassler, and T. C. Morrill, *Spectrometric Identification of Organic Compounds*. New York: Wiley, 1981.

[37] E. Kose, A. Atac, and F. Bardak, "The structural and spectroscopic investigation of 2-chloro-3-methylquinoline by DFT method and UV–Vis, NMR and vibrational spectral techniques combined with molecular docking analysis," *J. Mol. Struct.*, vol. 1163, pp. 147–160, Jul. 2018, doi: 10.1016/j.molstruc.2018.02.099.

[38] A. E. Ozel, S. Celik, and S. Akyuz, "Vibrational spectroscopic investigation of free and coordinated 5-aminoquinoline: The IR, Raman and DFT studies," *J. Mol. Struct.*, vol. 924, pp. 523–530, 2009, doi: 10.1016/j.molstruc.2008.12.065.

[39] G. Varsányi, *Assignments for vibrational spectra of 700 benzene derivatives*. Halsted Press, 1973.

[40] F. Bardak *et al.*, "Conformational, electronic, and spectroscopic characterization of isophthalic acid (monomer and dimer structures) experimentally and by DFT," *Spectrochim. Acta Part A Mol. Biomol. Spectrosc.*, vol. 165, pp. 33–46, Aug. 2016, doi: 10.1016/J.SAA.2016.03.050.

[41] V. Balachandran, M. Boobalan, M. Amaladasan, and S. Velmathi, "Synthesis and vibrational spectroscopic investigation of methyl l-prolinate hydrochloride: A computational insight," *Spectrosc. Lett.*, vol. 47, no. 9, pp. 676–689, 2014, doi: 10.1080/00387010.2013.834456.

[42] G. Socrates, *Infrared and Raman Characteristic Group Frequencies: Tables and Charts*. West Sussex, England: John Wiley & Sons Ltd., 2001.

[43] M. Arivazhagan and V. Krishnakumar, "Normal coordinate analysis of 1-chloroisoquinoline and 2-methyl-8-nitroquinoline," *Indian J. Pure Appl. Phys.*, vol. 43, no. August, pp. 573–578, 2005.

[44] H. Friebolin, *Basic One- and Two-Dimensional NMR Spectroscopy*. Wiley, 2005.

[45] H. O. Kalinowski, S. Berger, and S. Braun, *Carbon-13 NMR spectroscopy*. New York: Wiley, 1988.

[46] K. Pihlaja and E. Kleinpeter, *Carbon-13 NMR Chemical Shifts in Structural and Stereochemical Analysis*. VCH, 1994.

[47] E. Pretsch, P. Bühlmann, and C. Affolter, *Structure determination of organic compounds*, Fourth, Re., vol. 40, no. 3. Berlin, Heidelberg: Springer Berlin Heidelberg, 2009.

[48] P. O. Fort, D. C. G. a Pinto, C. M. M. Santos, and A. M. S. Silva, *Advanced NMR techniques for structural characterization of heterocyclic structures*, vol. 661, no. 2. 2007.

[49] D. Guillaumont and S. Nakamura, "Calculation of the absorption wavelength of dyes using time-dependent density-functional theory (TD-DFT)," *Dye. Pigment.*, vol. 46, no. 2, pp. 85–92, Aug. 2000, doi: 10.1016/S0143-7208(00)00030-9.

[50] A. Zangwill and P. Soven, "Density-functional approach to local-field effects in finite systems: Photoabsorption in the rare gases," *Phys. Rev. A*, vol. 21, no. 5, pp. 1561–1572, May 1980, doi: 10.1103/PhysRevA.21.1561.

[51] E. Runge and E. K. U. Gross, "Density-Functional Theory for Time-Dependent Systems," *Phys. Rev. Lett.*, vol. 52, no. 12, pp. 997–1000, Mar. 1984, Accessed: Mar. 26, 2014. [Online]. Available: http://prl.aps.org/abstract/PRL/v52/i12/p997_1.

[52] R. Hoffmann and R. B. Woodward, "The Conservation of Orbital Symmetry," *Acc. Chem. Res.*, vol. 1, no. 1, pp. 17–22, 1968, doi: 10.1021/ar50001a003.

[53] R. G. Parr and R. G. Pearson, "Absolute hardness: companion parameter to absolute electronegativity," *J. Am. Chem. Soc.*, vol. 105, no. 26, pp. 7512–7516, Dec. 1983, doi: 10.1021/ja00364a005.

[54] R. G. Parr, Y. Weitao, and W. Yang, *Density-Functional Theory of Atoms and Molecules*. Oxford University Press, USA, 1989.

[55] N. Okulik and A. H. Jubert, "Theoretical analysis of the reactive sites of non-steroidal anti-inflammatory drugs," *Internet Electron. J. Mol. Des.*, vol. 4, pp. 17–30, 2005, [Online]. Available: http://www.biochempress.com/av04_0017.html.

[56] F. J. Luque, J. M. López, and M. Orozco, "Perspective on 'Electrostatic interactions of a solute with a continuum. A direct utilization of ab initio molecular potentials for the prevision of solvent effects,'" *Theor. Chem. Accounts Theory, Comput. Model. (Theoretica Chim. Acta)*, vol. 103, no. 3–4, pp. 343–345, Feb. 2000, doi: 10.1007/s002149900013.

[57] R. S. Mulliken, "Electronic Population Analysis on LCAO-MO Molecular Wave Functions. I," *J. Chem. Phys.*, vol. 23, no. 10, pp. 1833–1840, 1955, doi: 10.1063/1.1740588.

[58] E. Kose, F. Bardak, and A. Atac, "The investigation of fluorine substitution in difluoroanilines with focus on 2,6-difluoroaniline by spectroscopic methods, density functional theory approach, and molecular docking," *J. Mol. Struct.*, vol. 1196, pp. 201–214, 2019, doi: 10.1016/j.molstruc.2019.06.038.